HHS Public Access

Author manuscript

J Invest Dermatol. Author manuscript; available in PMC 2022 June 01.

Published in final edited form as:

J Invest Dermatol. 2021 June ; 141(6): 1503–1511.e3. doi:10.1016/j.jid.2020.09.027.

DOCK8 expression in Treg cells maintains their stability and limits contact hypersensitivity

Hazel Wilkie[1], **Erin Janssen**[1], **Juan Manuel Leyva-Castillo**[1], **Raif S Geha**[1]

[1]Division of Immunology, Boston Children's Hospital and Department of Pediatrics Harvard Medical School, Boston, MA, USA

Abstract

Chronic dermatitis is a hallmark of Dedicator of cytokinesis 8 (DOCK8) deficiency. The migration of DOCK8-deficient T cells to the skin and their survival there has been reported to be defective. Surprisingly, we found that *Dock8*$^{-/-}$ mice demonstrated an exaggerated contact hypersensitivity (CHS) response to oxazolone (OXA) with increased ear swelling, T cell infiltration and expression of *Ifng*. To understand the mechanisms of persistent skin inflammation in DOCK8 deficiency, we examined mice with selective deficiency of DOCK8 in T cells or T regulatory cells (Tregs) and found that both have exaggerated CHS. Moreover, oral tolerance to OXA, mediated by Tregs, was impaired in *Dock8*$^{-/-}$ mice. Transfer of Tregs from OXA-sensitized WT, but not *Dock8*$^{-/-}$, mice reduced the CHS response of *Dock8*$^{-/-}$ recipients. Lack of DOCK8 in Tregs resulted in their acquisition of a pathogenic FOXP3^{+}T-bet^{+}IFNγ^{+} phenotype at CHS sites and promoted their conversion into ex-Treg cells. Transfer of Tregs from *Dock8*$^{-/-}$ mice increased the CHS response of WT recipients to OXA. Thus, DOCK8 expression in Tregs limits CHS by promoting Treg cell stability and fitness in inflamed skin. Interventions aimed at ameliorating Treg function may be useful in treating skin inflammation in DOCK8 deficiency.

Corresponding author: Raif S. Geha, Division of Immunology, Boston Children's Hospital, 1 Blackfan Circle, Karp Building 10th floor, Boston, MA, 02115, USA. Tel: (617) 919-2482; Fax: (617) 730-0528; raif.geha@childrens.harvard.edu.

Author Contributions

Conceptualization: EJ, JMLC, RSG
Data Curation: N/A
Formal Analysis: HW
Funding Acquisition: RSG
Investigation: HW, EJ, JMLC
Methodology: HW, EJ, JMLC, RSG
Project Administration: RSG
Resources: RSG
Software: N/A
Supervision: EJ, JMLC, RSG
Validation: HW, EJ, JMLC
Visualization: HW, RSG
Writing - Original Draft Preparation: HW, RSG
Writing - Review and Editing: HW, EJ, JMLC, RSG

Conflict of Interest

The authors have declared that no conflict of interest exists.

INTRODUCTION

Dedicator of cytokinesis 8 (DOCK8) deficiency is characterized by severe combined immunodeficiency, elevated IgE levels, food allergy and persistent skin inflammation, with predisposition to cutaneous viral, bacterial and fungal infections (Engelhardt et al., 2009; Zhang et al., 2009). The mechanism of persistent skin inflammation in DOCK8 deficiency remains unclear.

Contact hypersensitivity (CHS) is a mouse model of skin inflammation that mimics allergic contact dermatitis, to which T cells make a major contribution. In the sensitization phase of CHS, a topically applied hapten, such as oxazolone (OXA) or dinitrofluorobenzene (DNFB), is taken up by dendritic cells (DCs) in the skin, which migrate to the draining lymph nodes (LNs) where they present haptenated peptides to T cells, thereby initiating their activation and expansion (Christensen and Haase, 2012). Subsequent cutaneous challenge by application of hapten to a remote skin site causes the recruitment of circulating hapten-specific memory T cells and their local activation. Cytokine production by the recruited T cells upregulates local chemokine expression which causes skin infiltration by inflammatory cells and drives interstitial edema, resulting in swelling (Christensen and Haase, 2012). Acute CHS to OXA and DNFB is mediated predominantly by IFNγ produced by $CD4^+$ Th1 and $CD8^+$ T cells, with additional contributions by neutrophils and natural killer cells (Christensen and Haase, 2012).

$FOXP3^+$ T regulatory (Treg) cells are abundant in the skin (Ali and Rosenblum, 2017) and are critical for limiting cutaneous inflammation (Malhotra et al., 2018). Specifically, Tregs are required for contraction of the CHS response, as evidenced by prolonged skin inflammation in hapten-challenged ears of mice with induced deletion of Tregs (Lehtimaki et al., 2012). Furthermore, the induction of oral tolerance to hapten is dependent on Tregs (Desvignes et al., 2000). In an inflammatory milieu, Tregs may convert into cytokine-producing effector cells that can promote inflammation and lose expression of FOXP3 (Zhou et al., 2009).

The number and function of circulating Tregs are reduced in DOCK8 deficient patients (Janssen et al., 2014), and DOCK8 expression in Tregs is important for maintaining self-tolerance in mice (Janssen et al., 2017). Using the OXA-driven CHS model, we demonstrate that DOCK8 expression in Tregs is critical for maintaining Treg stability at sites of Type 1 cytokine mediated skin inflammation, suggesting that Treg dysfunction underlies the pathogenesis and persistence of skin inflammation in DOCK8 deficient patients.

RESULTS and DISCUSSION

Dock8$^{-/-}$ mice exhibit prolonged OXA-induced CHS.

Ear thickness at baseline was comparable between OXA-sensitized WT and *Dock8*$^{-/-}$ mice (Figure 1a). As expected, OXA challenge of WT mice caused an increase in ear thickness that peaked on Day 1 post-challenge, then gradually subsided over the next 5 days (Figure 1a). OXA challenge of *Dock8*$^{-/-}$ mice caused an increase in ear thickness that was comparable in the first 24 hours to that of WT controls, however, over the next 5 days, ear

thickness was significantly greater in *Dock8*$^{-/-}$ mice compared to WT controls (Figure 1a). There was no change in ear thickness in vehicle-challenged ears of *Dock8*$^{-/-}$ mice or WT controls at any time (Figure 1a). The exaggerated CHS response of *Dock8*$^{-/-}$ mice was not OXA specific. *Dock8*$^{-/-}$ mice sensitized and challenged with DNFB demonstrated exaggerated and prolonged ear swelling and thickness compared to WT controls (Figure S1a).

Histological examination of H&E stained ear sections revealed increased thickness, interstitial edema and cellular infiltration that were comparable at 24 hours post OXA challenge in *Dock8*$^{-/-}$ mice and WT controls (Figure 1b). These changes were markedly attenuated on Day 3 and subsided by Day 6 in WT controls but persisted through Day 6 in *Dock8*$^{-/-}$ mice (Figure 1b). Flow cytometry of ear cell suspensions demonstrated on Day 1 post OXA challenge, ears of WT mice had increased infiltration by CD45^{+} cells, including T cells, neutrophils and eosinophils (Figure 1c). Infiltration by T cells was still evident on Day 6, whereas neutrophil and eosinophil infiltration decreased on Day 3 and returned to baseline by Day 6 post challenge in WT mice (Figure 1c). Cellular infiltration was comparable in *Dock8*$^{-/-}$ mice and WT controls on Day 1 post challenge, however, cell numbers, including T cells, were significantly greater on Days 3 and 6 in *Dock8*$^{-/-}$ mice compared to WT controls (Figure 1c). There was no increase in cellular ear infiltrates over time in vehicle challenged ears of WT or *Dock8*$^{-/-}$ mice (Figure S1b).

The increased skin infiltration by T cells post-challenge was unexpected given DOCK8 activates CDC42 (cell division control protein 42), which is important for leukocyte actin reorganization and motility (Janssen et al., 2016) and a previous report found that DOCK8 deficient T cells have defective migration and survival in skin (Zhang et al., 2014). However, T cells accumulate in the spontaneous dermatitis lesions of *Dock8*$^{-/-}$ mice whose T cells express the AND TCR transgene (Yamamura et al., 2017). To rule out a migration defect, OXA-challenged ear skin explants were cultured overnight and cells that migrated out of the explants into the medium were counted. The percentage of CD45^{+} cells that migrated from ear skin explants into culture medium was comparable in *Dock8*$^{-/-}$ mice and WT controls (Figure S1c). This result suggests that the increased accumulation of CD45^{+} cells in OXA-challenged ears of *Dock8*$^{-/-}$ mice was not due to the inability of these cells to exit the skin.

The levels of *Ifng* and the IFNγ-inducible neutrophil- and T cell-attracting chemokine *Cxcl9* (Hartl et al., 2008; Qin et al., 1998) were strongly upregulated in WT mice on Days 1 and 3 and returned to baseline by Day 6 post challenge (Figure 1d). Expression of the IFNγ-inducible T cell- and eosinophil- attracting chemokine *Ccl5* (Kawka et al., 2014), was modestly upregulated on Day 1, but not Days 3 or 6, post-challenge in WT mice (Figure 1d). *Ifng, Cxcl9* and *Ccl5* levels in *Dock8*$^{-/-}$ mice were comparable to WT controls on Day 1, but were higher on Days 3 and 6 (Figure 1d). *Il13* was modestly upregulated only on Day 1 post challenge and was comparable in *Dock8*$^{-/-}$ mice and WT controls (Figure 1d). Recent work has revealed no defects in the phagocytic abilities of DOCK8 deficient neutrophils (Mandola et al., 2019), but studies on the function of DOCK8 deficient eosinophils are lacking. On day 1 post OXA challenge, ear infiltration by neutrophils and eosinophils was similar in *Dock8*$^{-/-}$ mice and WT controls (Figure 1c), therefore the ability of DOCK8 deficient neutrophils and eosinophils to migrate into the skin appears unaffected. The

increased accumulation of neutrophils and eosinophils in *Dock8*$^{-/-}$ mice on days 3 and 6 post challenge is likely due to the increased expression of the inflammatory chemokines CXCL9 and CCL5 respectively (Hartl et al., 2008; Kawka et al., 2014), thus these cells could be contributing to the exaggerated CHS response (Christensen and Haase, 2012). Collectively, the data indicate that DOCK8 deficiency results in prolonged Th1-dominated skin inflammation in OXA-driven CHS.

Selective deficiency of DOCK8 in T cells prolongs OXA-induced CHS.

To determine whether DOCK8 expression in T cells controls CHS, we examined *Cd4-Cre*^{tg}*Dock8*$^{flox/flox}$ mice, which lack DOCK8 expression selectively in T cells (Janssen et al., 2020). OXA-sensitized *Cd4-Cre*^{tg}*Dock8*$^{flox/flox}$ mice demonstrated significantly increased ear thickness (Figure S2a), increased interstitial edema and cell infiltration (Figure S2b) with increased CD45^{+} cells, CD4^{+} T cells, CD8^{+} T cells, neutrophils and eosinophils (Figure S2c) and increased expression of *Ifng, Cxcl9* and *Ccl5* (Figure S2d) for 6 Days post-OXA challenge compared to *Cd4-Cre*^{tg}*Dock8*$^{+/+}$ controls.

There are subsets of CD4^{+} colonic macrophages (Schridde et al., 2017) and splenic DCs (Sichien et al., 2017) whose function could be affected by loss of DOCK8 expression (Harada et al., 2012). However, *Cd4-Cre*^{tg}*Dock8*$^{flox/flox}$ mice respond to OXA similarly to mice with selective deletion of DOCK8 in Tregs (see below) indicating that CD4^{+} cell subsets other than T cells contribute minimally, if at all, to the exaggerated CHS in *Cd4-Cre*^{tg}*Dock8*$^{flox/flox}$ mice. Thus, the data strongly suggest that DOCK8 expression in T cells limits the magnitude and duration of skin inflammation in CHS.

Selective deficiency of DOCK8 in Tregs prolongs OXA-induced CHS.

Cd4-Cre^{tg}*Dock8*$^{flox/flox}$ mice lack DOCK8 in both T effector (Teff) and Treg cells. To directly assess the role of DOCK8 expression in Tregs in controlling CHS to OXA, we examined mice with selective deficiency of DOCK8 in Tregs. *Foxp3*$^{YFP\text{-}cre}$*Dock8*$^{flox/flox}$ mice exhibited significantly increased ear thickness for over 6 Days post OXA challenge compared to *Foxp3*$^{YFP\text{-}cre}$*Dock8*$^{+/+}$ controls (Figure S3a). *Foxp3*$^{YFP\text{-}cre}$*Dock8*$^{flox/flox}$ mice suffer from autoimmunity (Janssen et al., 2017) which might have confounded the results. To circumvent this limitation, we generated *Foxp3*$^{eGFP\text{-}cre\text{-}ERT2}$*Dock8*$^{flox/flox}$ mice that carry a tamoxifen-inducible *Cre* gene in the *Foxp3* locus. These mice remain healthy with no evidence of systemic or skin inflammation. *Foxp3*$^{eGFP\text{-}cre\text{-}ERT2}$*Dock8*$^{flox/flox}$ mice and *Foxp3*$^{eGFP\text{-}cre\text{-}ERT2}$*Dock8*$^{+/+}$ controls were treated with tamoxifen for 17 Days during which time they were sensitized (Day 9) and challenged with OXA (Day 14), then sacrificed 3 days post challenge (Figure 2a). Immunoblotting revealed that DOCK8 expression in Tregs from tamoxifen treated *Foxp3*$^{eGFP\text{-}cre\text{-}ERT2}$*Dock8*$^{flox/flox}$ mice was significantly reduced to ~40% of its level in Tregs of *Foxp3*$^{eGFP\text{-}cre\text{-}ERT2}$*Dock8*$^{+/+}$ controls (Figure 2b). There was no reduction of DOCK8 expression in CD4^{+}FOXP3^{-}(GFP^{-}) Teff cells from *Foxp3*$^{eGFP\text{-}cre\text{-}ERT2}$*Dock8*$^{flox/flox}$ mice compared to Teff cells from controls.

Ear thickness post OXA challenge in *Foxp3*$^{eGFP\text{-}cre\text{-}ERT2}$*Dock8*$^{flox/flox}$ mice was significantly increased compared to *Foxp3*$^{eGFP\text{-}cre\text{-}ERT2}$*Dock8*$^{+/+}$ controls (Figure 2c). Histological analysis revealed increased thickening, interstitial edema, and cellular

infiltration in OXA-challenged ears of *Foxp3*$^{eGFP\text{-}cre\text{-}ERT2}$*Dock8*$^{flox/flox}$ mice compared to controls (Figure 2d). The numbers of CD45$^+$ cells, total CD4$^+$ T cells, CD8$^+$ T cells, neutrophils and eosinophils, as well as expression of *Ifng, Cxcl9* and *Ccl5* were significantly higher in OXA-challenged ears of *Foxp3*$^{eGFP\text{-}cre\text{-}ERT2}$*Dock8*$^{flox/flox}$ mice compared to controls (Figure 2e, f).

To further demonstrate that DOCK8 expression confers on Tregs the capacity to suppress CHS, we examined the ability of adoptively transferred DOCK8 sufficient Tregs to suppress the exaggerated CHS of *Dock8*$^{-/-}$ mice. Tregs were isolated from the skin draining LNs of OXA-sensitized WT mice and *Dock8*$^{-/-}$ controls and transferred intra-dermally into the ears of OXA-sensitized *Dock8*$^{-/-}$ recipients. The injected ears were immediately challenged with OXA and ear thickness was measured for 6 Days post-challenge. *Dock8*$^{-/-}$ mice that received WT Tregs had significantly reduced ear thickness compared to *Dock8*$^{-/-}$ mice that received *Dock8*$^{-/-}$ Tregs or PBS (Figure 2g). These results suggest that DOCK8 expression in Tregs is critical for restraining inflammation at CHS sites, and that immunotherapy with WT Tregs may be useful in dampening skin inflammation in DOCK8 deficiency.

Oral tolerance to hapten is impaired in *Dock8*$^{-/-}$ mice.

Orally induced tolerance to hapten is dependent on Tregs (Desvignes et al., 2000), therefore, we examined the induction of oral tolerance to OXA in *Dock8*$^{-/-}$ mice. Mice were gavaged daily for 3 Days with OXA or olive oil vehicle, prior to OXA sensitization and challenge and were sacrificed on Day 3 post challenge (Figure 3a). As expected, OXA gavage markedly reduced ear thickness post-OXA challenge compared to vehicle gavage in WT mice (Figure 3b). In contrast, there was no significant reduction of ear thickness post-challenge in *Dock8*$^{-/-}$ mice (Figure 3b). Histological analysis of OXA-challenged ears revealed reduced thickness, interstitial edema and cellular infiltration in OXA-gavaged WT, but not *Dock8*$^{-/-}$, mice compared to vehicle-gavaged controls (Figure 3c). There was also significantly reduced infiltration by CD45$^+$ cells, CD8$^+$ T cells and neutrophils as well as significantly decreased expression of *Ifng, Cxcl9* and *Ccl5* expression in OXA-gavaged WT, but not *Dock8*$^{-/-}$, mice compared to vehicle-gavaged controls (Figure 3d, e). Collectively, these data indicate that oral tolerance is impaired in DOCK8 deficiency. Impaired oral tolerance may contribute to the susceptibility of DOCK8 deficient patients to food allergy (Happel et al., 2016).

DOCK8 maintains Treg stability and fitness at sites of CHS driven skin inflammation.

The numbers of CD4$^+$FOXP3$^-$(GFP$^-$) Teff and CD4$^+$FOXP3$^+$(GFP$^+$) Treg cells increased post OXA challenge in tamoxifen-treated *Foxp3*$^{eGFP\text{-}cre\text{-}ERT2}$*Dock8*$^{flox/flox}$ mice and *Foxp3*$^{eGFP\text{-}cre\text{-}ERT2}$*Dock8*$^{+/+}$ controls (Figure 4a). However, the numbers of Teff cells in OXA-challenged ears were significantly higher in *Foxp3*$^{eGFP\text{-}cre\text{-}ERT2}$*Dock8*$^{flox/flox}$ mice compared to controls (Figure 4a, left), whereas the number of Tregs was comparable in the two strains (Figure 4a, middle). Consequently, the percentage of Tregs among CD4$^+$ T cells was significantly lower in *Foxp3*$^{eGFP\text{-}cre\text{-}ERT2}$*Dock8*$^{flox/flox}$ mice compared to controls (Figure 4a, right). This relative depletion of Tregs was not due to increased cell death or reduced proliferation as the percentages of Caspase3$^+$ cells (Figure 4b), 7AAD$^+$AnnexinV$^+$ cells (Figure S3b) and Ki67$^+$ cells (Figure 4c) among CD4$^+$FOXP3$^+$(GFP$^+$) Tregs in OXA-

challenged ears were comparable between *Foxp3*$^{eGFP\text{-}cre\text{-}ERT2}$*Dock8*$^{flox/flox}$ mice and controls.

During Type 1 inflammation, Tregs increase expression of T-bet which enables their migration into sites of IFNγ-mediated inflammation while maintaining their suppressive capability (Georgiev et al., 2019). During chronic or intense inflammation, Tregs further increase expression of T-bet leading to IFNγ production with a concomitant decrease, and in some cells eventual cessation, of FOXP3 expression to become ex-Tregs (Oldenhove et al., 2009), contributing to tissue inflammation (Duarte et al., 2009; Zhou et al., 2009). The percentage of T-bet^{+}IFNγ^{+} cells among FOXP3^{+} cells in both vehicle- and OXA-challenged skin was increased in *Foxp3*$^{eGFP\text{-}cre\text{-}ERT2}$*Dock8*$^{flox/flox}$ mice compared to controls (Figure 4d). IFNγ expression was concordant with T-bet expression (Figure S3c). The mean fluorescence intensity (MFI) of FOXP3 was significantly reduced in FOXP3^{+}T-bet^{+}IFNγ^{+} Tregs from OXA-challenged skin of *Foxp3*$^{eGFP\text{-}cre\text{-}ERT2}$*Dock8*$^{flox/fox}$ mice compared to controls (Figure 4e). The results demonstrate that DOCK8 expression in Tregs restrains their acquisition of an inflammatory phenotype at sites of Th1-mediated skin inflammation.

On day 3 post OXA challenge, the phenotype of Tregs from the skin draining LNs of tamoxifen-treated *Foxp3*$^{eGFP\text{-}cre\text{-}ERT2}$*Dock8*$^{flox/flox}$ mice and controls was analyzed. Tregs from *Foxp3*$^{eGFP\text{-}cre\text{-}ERT2}$*Dock8*$^{flox/fox}$ mice demonstrated reduced expression of the suppressive markers PD-1 and LAP, which binds TGFβ on the cell surface (Figure S3d, e), Helios (Figure S3f), a marker of thymus-derived FOXP3-stable nTregs (Georgiev et al., 2019), and CD103 (Figure S3g), an integrin required for retention in the skin that is also linked with Treg suppressive activity (Braun et al., 2015). There was no difference in the expression of IL-10 or the suppressive marker ILT3 (Harakal et al., 2016) in DOCK8 deficient Tregs (Figure S3h, i). The reduced suppressive function and unstable phenotype of DOCK8 deficient Treg cells could contribute to the expansion of Teff cells at CHS sites in mice with DOCK8 deficient Tregs.

To determine if DOCK8 deficient Tregs are pathogenic, we transferred 1×10^{6} CD4^{+}FOXP3^{+} (GFP^{+})CD25^{+} Tregs from naïve *Foxp3*^{eGFP}*Dock8*$^{-/-}$ or *Foxp3*^{eGFP}*Dock8*$^{+/+}$ donors into WT recipients, prior to OXA sensitization and subsequent challenge. Recipients of *Dock8*$^{-/-}$ Tregs had significantly increased ear thickness and *Ifng* expression compared to recipients of WT Tregs post-OXA challenge (Figure 4f, g). These results indicate that Tregs contribute to the increased skin inflammation at CHS sites in DOCK8 deficiency.

Given the reduced expression of FOXP3 in DOCK8 deficient FOXP3^{+}T-bet^{+}IFNγ^{+} Tregs, we also evaluated whether DOCK8 deficient Tregs have increased propensity to convert into ex-Tregs at sites of CHS inflammation. We generated *Foxp3*$^{eGFP\text{-}cre\text{-}ERT2}$*R26*$^{eYFP/eYFP}$*Dock8*$^{flox/flox}$ mice and *Foxp3*$^{eGFP\text{-}cre\text{-}ERT2}$*R26*$^{eYFP/eYFP}$*Dock8*$^{+/+}$ controls. In these FOXP3 lineage tracing mice, CD4^{+}GFP^{+}YFP^{+} Tregs that lose FOXP3(GFP) expression to become ex-Tregs can be traced as CD4^{+}GFP^{-}YFP^{+} cells due to their continued expression of YFP. The mice were tamoxifen-treated, OXA-sensitized and challenged following the protocol in Figure 2a. The numbers of CD4^{+}GFP^{-}YFP^{+} ex-Tregs in vehicle-challenged ears of *Foxp3*$^{eGFP\text{-}cre\text{-}ERT2}$*R26*$^{eYFP/eYFP}$*Dock8*$^{flox/flox}$ mice and controls were negligible, but

increased significantly with OXA challenge in both strains (Figure 4h), consistent with previous observations that Tregs are driven to instability in an inflammatory milieu (Feng et al., 2014; Janssen et al 2017). Importantly, the number of $CD4^+GFP^-YFP^+$ ex-Tregs, as well as their percentage among $CD4^+YFP^+$ cells, were significantly higher in OXA-challenged ears of *Foxp3*$^{eGFP\text{-}cre\text{-}ERT2}$*R26*$^{eYFP/eYFP}$*Dock8*$^{flox/flox}$ mice compared to controls (Figure 4h). These results indicate that DOCK8 expression in Tregs is important for maintaining the stability of FOXP3 expression at sites of CHS inflammation.

Stable FOXP3 expression and function in Tregs depends on IL-2 driven phosphorylation of STAT5 (Duarte et al., 2009). pSTAT5 binding to the intronic CNS2 regulatory element of the *Foxp3* gene cooperatively enhances the binding of pSTAT5 to the *Foxp3* promoter, thereby maintaining *Foxp3* expression in dividing and activated Tregs at sites of tissue inflammation (Feng et al., 2014). DOCK8 interacts with STAT5 and enhances IL-2 driven STAT5 phosphorylation in Tregs (Janssen et al., 2017; Shi et al., 2018). Defective IL-2 driven STAT5 phosphorylation in DOCK8 deficient Tregs may result in their instability and subversion into effector T cells that contribute to the exaggerated CHS response, resulting in unrestrained Type 1 skin inflammation. Interventions aimed at ameliorating Treg function may be useful in treating skin inflammation in DOCK8 deficiency.

MATERIALS AND METHODS

Further information can be found in Supplemental Methods and in Supplemental Figures.

Mice.

Wild type (WT) C57BL/6 mice (Charles River, Worcester, MA), *Foxp3*$^{eGFP\text{-}cre\text{-}ERT2}$ (*Foxp3*$^{tm9(EGFP/cre/ERT2)Ayr}$/J; 016961), R26-stop-eYFP (*B6.129X1-Gt(ROSA)26Sor*$^{tm1(EYFP)Cos}$/J; 006148), *Foxp3*^{eGFP} (*C.Cg-Foxp3*^{tm2Tch}/J; 006769) mice (all from Jackson Laboratory, Bar Harbor, ME) and *Cd4-Cre* transgenic mice (4196; Taconic Biosciences, Albany, NY) were purchased. Generation of *Dock8*$^{-/-}$ (Janssen et al., 2016), *Dock8*$^{flox/flox}$ (Janssen et al., 2017), *Foxp3*$^{YFP\text{-}cre}$*Dock8*$^{flox/flox}$ (Janssen et al., 2017) and *Cd4-Cre*^{tg}*Dock8*$^{flox/flox}$ (Janssen et al., 2020) mice is previously described. Strains were crossed to generate *Foxp3*$^{eGFP\text{-}cre\text{-}ERT2}$*Dock8*$^{flox/flox}$, *Foxp3*^{eGFP}*Dock8*$^{-/-}$ and *Foxp3*$^{eGFP\text{-}cre\text{-}ERT2}$*R26*$^{eYFP/eYFP}$*Dock8*$^{flox/flox}$ mice. Age and sex matched male and female adult (> 6 weeks old) mice were used for experiments. Individual experiments were repeated at least 3 times. All mice were housed in a specific pathogen-free environment. All procedures performed were in accordance with the Animal Care and Use Committee of Boston Children's Hospital.

Contact Hypersensitivity.

Mice were sensitized with 100 μl 2% OXA (4-Ethoxymethylene-2-phenyl-2-oxazolin-5-one) (Millipore Sigma, Burlington, MA) in 100% ethanol on shaved abdomens then challenged 5-6 days later with 25 μl 0.5% OXA in 100% ethanol on the right ear and 25 μl 100% ethanol (vehicle) on the left ear. Mice were sensitized with 50 μl 0.5% DNFB (1-fluoro-2,4-dinitrobenzene; Millipore Sigma) in acetone:oil (4:1) on shaved abdomens then challenged 5 days later with 25 μl 0.5% DNFB in acetone:oil (4:1) on the right ear and 25 μl acetone:oil

(4:1) (vehicle) on the left ear. Ear thickness was measured with a micrometer before challenge and every 24 hours thereafter until euthanasia. To induce oral tolerance to OXA-driven CHS, mice received 300 μl 0.5% OXA in olive oil P.O. daily for 3 days ending 5 days before OXA sensitization. Non-tolerized mice received olive oil.

Histology.

Ear tissue samples were preserved in 10% formalin before paraffin embedding and hematoxylin and eosin (H&E) staining. A Nikon Eclipse E800 microscope at 10x or 20x objective with camera (Nikon DS-Ri1) was used for image capture.

Extra-Cellular Staining of Cells for Flow Cytometry.

Single cell suspensions from murine ears and draining LNs were prepared as described previously (Malhotra et al., 2018). Digested tissue was filtered, washed and resuspended in Fcγ receptor-specific blocking Ab (clone 93) then incubated with fluorochrome-conjugated Abs against CD45.2 (104), CD3 (17A2), CD4 (RM4-5), CD25 (PC61), CD8 (53-6.7), CD11b (M1/70), GR1 (RB6-8C5), PD-1 (29F.1A12), LAP (TW7-16B4), CD103 (2E7), ILT3 (H1.1) (all BioLegend, San Diego, CA), SiglecF (E50-2440; BD Pharmagen, San Jose, CA) and fixable viability dye (Thermo Fisher, Waltham, MA).

Intra-Cellular Staining of Cells for Flow Cytometry.

For transcription factor staining, cells were treated as above then fixed and permeabilized with the eBioscience™ Intracellular Fixation and Permeabilization Buffer Set (Invitrogen) and incubated with fluorochrome-conjugated antibodies against FOXP3 (150D/E4; Thermo Fisher), active-Caspase-3 (C92-605; BD Pharmagen), Ki67 (16A8; BioLegend), Helios (22F6; BioLegend). For intra-cellular cytokine staining, a single cell suspension of cells was stimulated (Janssen et al., 2017), stained, fixed and permeabilized as above then incubated with fluorochrome-conjugated antibodies against FOXP3, T-bet (4B10; BioLegend), IFNγ (XMG1.2; Thermo Fisher), IL-10 (JES5-16E3; BioLegend). Cell counts of skin samples were determined by addition of Precision Count Beads™ (BioLegend) to samples immediately prior to flow cytometry. A BD LSRFortessa cell analyzer with FACSDiva software (BD Biosciences, San Jose, CA) was used to collect all data which was analyzed using FlowJo v10 (Tree Star Inc., San Jose, CA).

Skin preparation for RNA extraction and RT-qPCR.

RNA was extracted from homogenized ear tissue using RNAqueous Phenol-free total RNA Isolation kit (Thermo Fisher). cDNA was synthesized using iScript™ cDNA Synthesis Kit (Bio-Rad Laboratories, Hercules, CA). RT-qPCR was performed with TaqMan® Universal Master Mix II and TaqMan Probes using a QuantStudio 3 Real-Time PCR machine (all Thermo Fisher). Cytokine expression was normalized to β2-*microglobulin* using the $2^{-\Delta\Delta Ct}$ method. For each gene, the mean expression of WT vehicle ear was set to 1 for fold change calculations.

DOCK8 Immunoblot of Sorted Tregs.

Splenocytes were lysed with ACK Lysis Buffer (Sigma-Aldrich, Burlington, MA), enriched using MACS $CD4^+$ T Cell Isolation Kit (Miltenyi Biotec, Somerville, MA), then stained for CD4, CD25 and CD39 (Duha59; BioLegend). Cells were sorted using a BD FACSAria with FACSDiva software (BD Biosciences) to collect Teffs ($CD4^+GFP^-CD25^-CD39^-$) and Tregs ($CD4^+GFP^+CD25^+CD39^+$). Sorted cells were lysed in 1% Triton buffer (150 mM NaCl, 25 mM Tris-Cl, pH 7.5, 5 mM EDTA) containing complete protease inhibitors (Roche, Sigma-Aldrich, Burlington, MA). Total cell lysates were separated by SDS-PAGE and transferred to nitrocellulose membranes. Antibodies used for Western Blot were anti-DOCK8 (H159, Santa Cruz, Dallas, TX) and anti-STAT3 (79D7, Cell Signaling, Danvers, MA). Image J 1.51s software (US National Institutes of Health) was used to analyze band densitometry.

Adoptive Transfer into *Dock8*$^{-/-}$ mice.

On day 6 post OXA-sensitization, skin draining lymph nodes were isolated and a single cell suspension of lymphocytes was sorted using MACS $CD4^+CD25^+$ Regulatory T Cell Isolation Kit (Miltenyi Biotec). 5,000 WT or *Dock8*$^{-/-}$ Tregs or 20 µl PBS were transferred intra-dermally into the ears of OXA-sensitized *Dock8*$^{-/-}$ recipients. Recipient ears were immediately challenged with OXA and ear thickness was measured for 6 days.

Adoptive Transfer into WT mice.

$CD4^+$ T cells were sorted using MACS $CD4^+$ T Cell Isolation Kit (Miltenyi Biotec) from naïve *Foxp3*^{eGFP}*Dock8*$^{-/-}$ and *Foxp3*^{eGFP}*Dock8*$^{+/+}$ mice. $CD4^+$ T cells were stained for CD3, CD4 and CD25. Tregs were sorted using a MA900 Sorter (Sony, San Jose, CA) with Sony Sorter Software version 3.0.5 (Sony). $1x10^6$ *Dock8*$^{-/-}$ or WT Tregs were transferred intra-venously into naïve WT mice which were immediately OXA-sensitized then challenged with OXA (right ear) and vehicle (left ear) as above. Ear thickness was measured for 6 days post challenge.

Tamoxifen treatment.

Tamoxifen (Sigma-Aldrich) was dissolved in corn oil and incubated at 37°C, 240 rpm for 2 hours before intra-peritoneal injection. 3 mg tamoxifen per day was injected on days 0-4. Subsequently, mice received 5 mg tamoxifen every 3 days to maintain the phenotype. CHS experiments began after 9 days of tamoxifen treatment.

Statistical analysis.

Data were analyzed for statistical significance using GraphPad Prism 8.0 (GraphPad Software, San Diego, CA) using unpaired 2-tailed Student's *t* test, 1-way ANOVA with Tukey's multiple comparisons test or 2-way ANOVA with Sidak's multiple comparison test depending on the number of groups/days. The threshold for significance was $P\ value < 0.05$. Observed statistical power (> 0.8 for all analyses) was calculated using SPSS 24 (IBM), using alpha = 0.05.

Data Availability Statement

No datasets were generated or analyzed during this study.

Supplementary Material

Refer to Web version on PubMed Central for supplementary material.

Acknowledgments

We thank the Harvard Rodent Histopathology and Flow Cytometry core at Boston Children's Hospital; P. Coblentz for technical assistance; Drs. H. Oettgen and T. Chatila for reading the manuscript and useful discussions. This work was supported by NIH grants USPHS RO1AI114588 (R.S.G.), K08AI114968 (E.J.), J.-M.L.-C. is supported by NIAID T32 training grant (5T32AI007512).

Abbreviations used throughout the text:

CHS	contact hypersensitivity
DOCK8	Dedicator of cytokinesis 8
OXA	Oxazolone
Treg	T regulatory cell
Teff	T effector cell

REFERENCES

Ali N, Rosenblum MD Regulatory T cells in the skin. Immunology 2017; 152, 372–381. [PubMed: 28699278]

Braun A, Dewert N, Brunnert F, Schnabel V, Hardenberg JH, Richter B, et al. Integrin alphaE(CD103) Is Involved in Regulatory T-Cell Function in Allergic Contact Hypersensitivity. J Invest Dermatol 2015; 135, 2982–2991. [PubMed: 26203637]

Christensen AD, Haase C Immunological mechanisms of contact hypersensitivity in mice. APMIS 2012; 120, 1–27. [PubMed: 22151305]

Desvignes C, Etchart N, Kehren J, Akiba I, Nicolas JF, Kaiserlian D Oral Administration of Hapten Inhibits In Vivo Induction of Specific Cytotoxic CD8+ T Cells Mediating Tissue Inflammation: A Role for Regulatory CD4+ T Cells. J Immunol 2000; 164, 2515–2522. [PubMed: 10679089]

Duarte JH, Zelenay S, Bergman ML, Martins AC, Demengeot J Natural Treg cells spontaneously differentiate into pathogenic helper cells in lymphopenic conditions. Eur J Immunol 2009; 39, 948–955. [PubMed: 19291701]

Engelhardt KR, McGhee S, Winkler S, Sassi A, Woellner C, Lopez-Herrera G, et al. Large deletions and point mutations involving the dedicator of cytokinesis 8 (DOCK8) in the autosomal-recessive form of hyper-IgE syndrome. J Allergy Clin Immunol 2009; 124, 1289–1302. [PubMed: 20004785]

Feng Y, Arvey A, Chinen T, van der Veeken J, Gasteiger G, Rudensky AY Control of the inheritance of regulatory T cell identity by a cis element in the Foxp3 locus. Cell 2014; 158, 749–763. [PubMed: 25126783]

Georgiev P, Charbonnier LM, Chatila T Regulatory T cells: the many faces of Foxp3. J Clin Immunol 2019; 39, 623–640. [PubMed: 31478130]

Happel CS, Stone KD, Freeman AF, Shah NN, Wang A, Lyons JJ, et al. Food allergies can persist after myeloablative hematopoietic stem cell transplantation in dedicator of cytokinesis 8-deficient patients. J Allergy Clin Immunol 2016; 137, 1895–1898 e1895. [PubMed: 26827248]

Harada Y, Tanaka Y, Terasawa M, Pieczyk M, Habiro K, Katakai T, et al. DOCK8 is a Cdc42 activator critical for interstitial dendritic cell migration during immune responses. Blood 2012; 119, 4451–4461. [PubMed: 22461490]

Harakal J, Rival C, Qiao H, Tung KS Regulatory T Cells Control Th2-Dominant Murine Autoimmune Gastritis. J Immunol 2016; 197, 27–41. [PubMed: 27259856]

Hartl D, Krauss-Etschmann S, Koller B, Hordijk PL, Kuijpers TW, Hoffmann F, et al. Infiltrated Neutrophils Acquire Novel Chemokine Receptor Expression and Chemokine Responsiveness in Chronic Inflammatory Lung Diseases. J Immunol 2008; 181, 8053–8067. [PubMed: 19017998]

Janssen E, Kumari S, Tohme M, Ullas S, Barrera V, Tas JM, et al. DOCK8 enforces immunological tolerance by promoting IL-2 signaling and immune synapse formation in Tregs. JCI Insight 2017; 2, (19):e94298.

Janssen E, Morbach H, Ullas S, Bannock JM, Massad C, Menard L et al. Dedicator of cytokinesis 8-deficient patients have a breakdown in peripheral B-cell tolerance and defective regulatory T cells. J Allergy Clin Immunol 2014; 134, 1365–1374. [PubMed: 25218284]

Janssen E, Tohme M, Butts J, Giguere SS, Sage PT, Velazquez FE, et al. DOCK8 is essential for LFA-1 dependent positioning of T follicular helper cells in germinal centers. JCI Insight 2020.

Janssen E, Tohme M, Hedayat M, Leick M, Kumari S, Ramesh N, et al. A DOCK8-WIP-WASp complex links T cell receptors to the actin cytoskeleton. J Clin Invest 2016; 126, 3837–3851. [PubMed: 27599296]

Kawka E, Witowski J, Fouqet N, Tayama H, Bender TO, Catar R, et al. Regulation of chemokine CCL5 synthesis in human peritoneal fibroblasts: a key role of IFNg. Mediators Inflamm 2014; 2014, 590654. [PubMed: 24523572]

Lehtimaki S, Savinko T, Lahl K, Sparwasser T, Wolff H, Lauerma A, et al. The temporal and spatial dynamics of FOXP3+ Treg cell-mediated suppression during Contact Hypersensitivity responses in a murine model. J Invest Dermatol 2012; 132, 2744–2751. [PubMed: 22739792]

Malhotra N, Leyva-Castillo JM, Jadhav U, Barreiro O, Kam C, O'Neill NK, et al. RORa-expressing T regulatory cells restrain allergic skin inflammation. Science Immunology 2018; 3.

Mandola AB, Levy J, Nahum A, Hadad N, Levy R, Rylova A, et al. Neutrophil functions in Immunodeficiency due to DOCK8 deficiency. Immunol Invest 2019; 48, 431–439. [PubMed: 30689480]

Oldenhove G, Bouladoux N, Wohlfert EA, Hall JA, Chou D, Dos Santos L et al. Decrease of Foxp3+ Treg cell number and acquisition of effector cell phenotype during lethal infection. Immunity 2009; 31, 772–786. [PubMed: 19896394]

Qin S, Rottman JB, Myers P, Kassam N, Weinblatt M, Loetscher M et al. The chemokine receptors CXCR3 and CCR5 mark subsets of T cells associated with certain inflammatory reactions. J Clin Invest 1998; 101, 746–754. [PubMed: 9466968]

Schridde A, Bain CC, Mayer JU, Montgomery J, Pollet E, Denecke B et al. Tissue-specific differentiation of colonic macrophages requires TGFbeta receptor-mediated signaling. Mucosal Immunol 2017; 10, 1387–1399. [PubMed: 28145440]

Shi H, Liu C, Tan H, Li Y, Nguyen TM, Dhungana Y et al. Hippo Kinases Mst1 and Mst2 Sense and Amplify IL-2R-STAT5 Signaling in Regulatory T Cells to Establish Stable Regulatory Activity. Immunity 2018; 49, 899–914 e896. [PubMed: 30413360]

Sichien D, Lambrecht BN, Guilliams M, Scott CL Development of conventional dendritic cells: from common bone marrow progenitors to multiple subsets in peripheral tissues. Mucosal Immunol 2017; 10, 831–844. [PubMed: 28198365]

Yamamura K, Uruno T, Shiraishi A, Tanaka Y, Ushijima M, Nakahara T, et al. The transcription factor EPAS1 links DOCK8 deficiency to atopic skin inflammation via IL-31 induction. Nat Commun 2017; 8, 13946. [PubMed: 28067314]

Zhang Q, Davis JC, Lamborn IT, Freeman AF, Jing H, Favreau AJ, et al. Combined Immunodeficiency Associated with DOCK8 mutations. N Engl J Med 2009; 361, 2046–2055. [PubMed: 19776401]

Zhang Q, Dove CG, Hor JL, Murdock HM, Strauss-Albee DM, Garcia JA, et al. DOCK8 regulates lymphocyte shape integrity for skin antiviral immunity. J Exp Med 2014; 211, 2549–2566. [PubMed: 25422492]

Zhou X, Bailey-Bucktrout SL, Jeker LT, Penaranda C, Martinez-Llordella M, Ashby M et al. Instability of the transcription factor Foxp3 leads to the generation of pathogenic memory T cells in vivo. Nat Immunol 2009; 10, 1000–1007. [PubMed: 19633673]

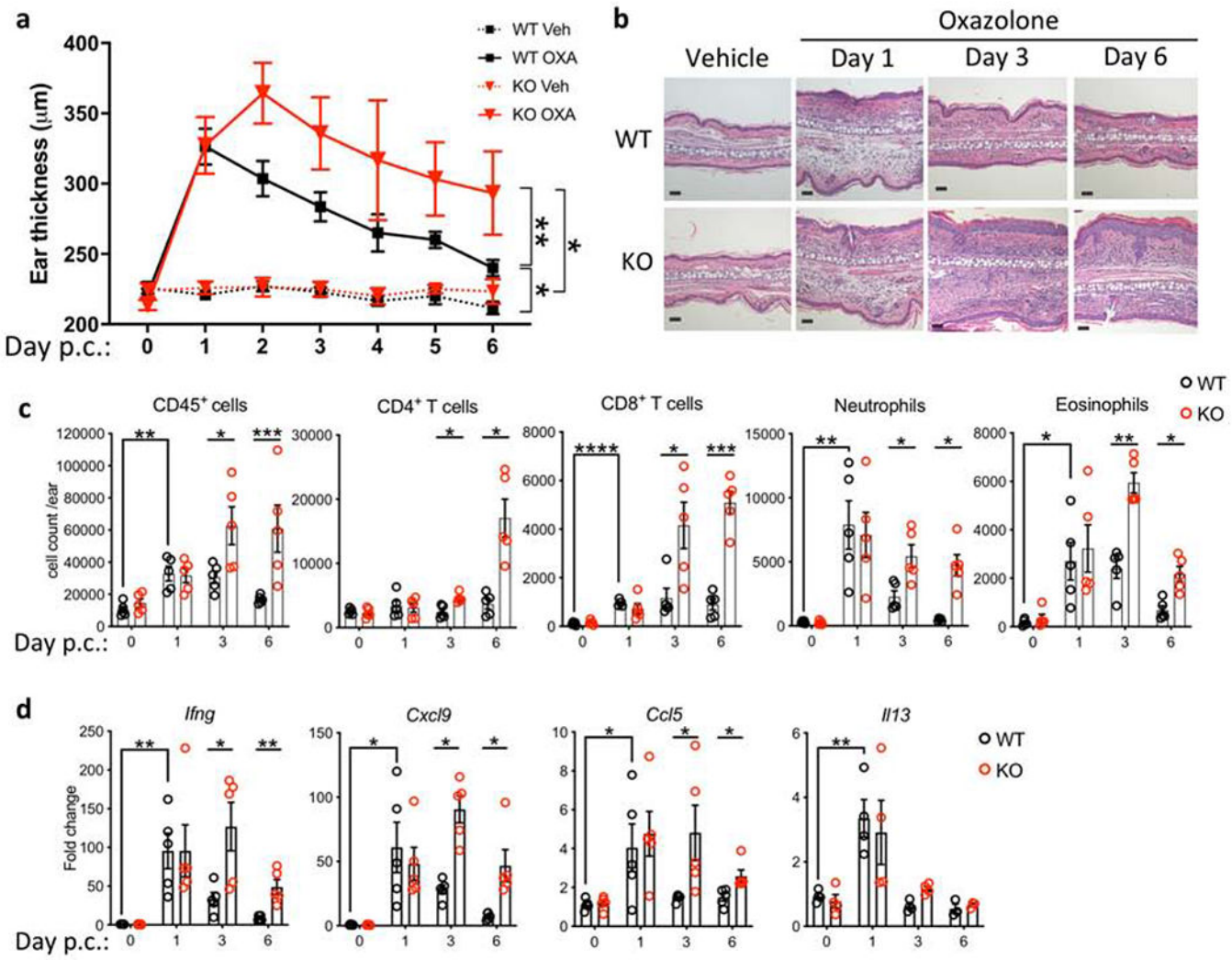

Figure 1. Prolonged CHS to oxazolone in *Dock8*$^{-/-}$ mice.

(**a**) Ear thickness post challenge (p.c.) with OXA or vehicle in *Dock8*$^{-/-}$ (KO) mice and WT controls. (**b**) Representative photomicrographs of H&E stained sections from ears challenged with vehicle or OXA. Scale bars: 50 μm. (**c** and **d**) Cellular infiltration (**c**) and cytokine and chemokine expression relative to the mean of WT Day 0 (**d**) in ears post challenge. Symbols represent individual mice (n=4-5/time-point), bars display mean ± SEM. * p <0.05, ** p <0.01, *** p <0.001, **** p <0.0001, by 2-way ANOVA for global significance (**a**) with Sidak's multiple comparison test for differences between days (**c**, **d**).

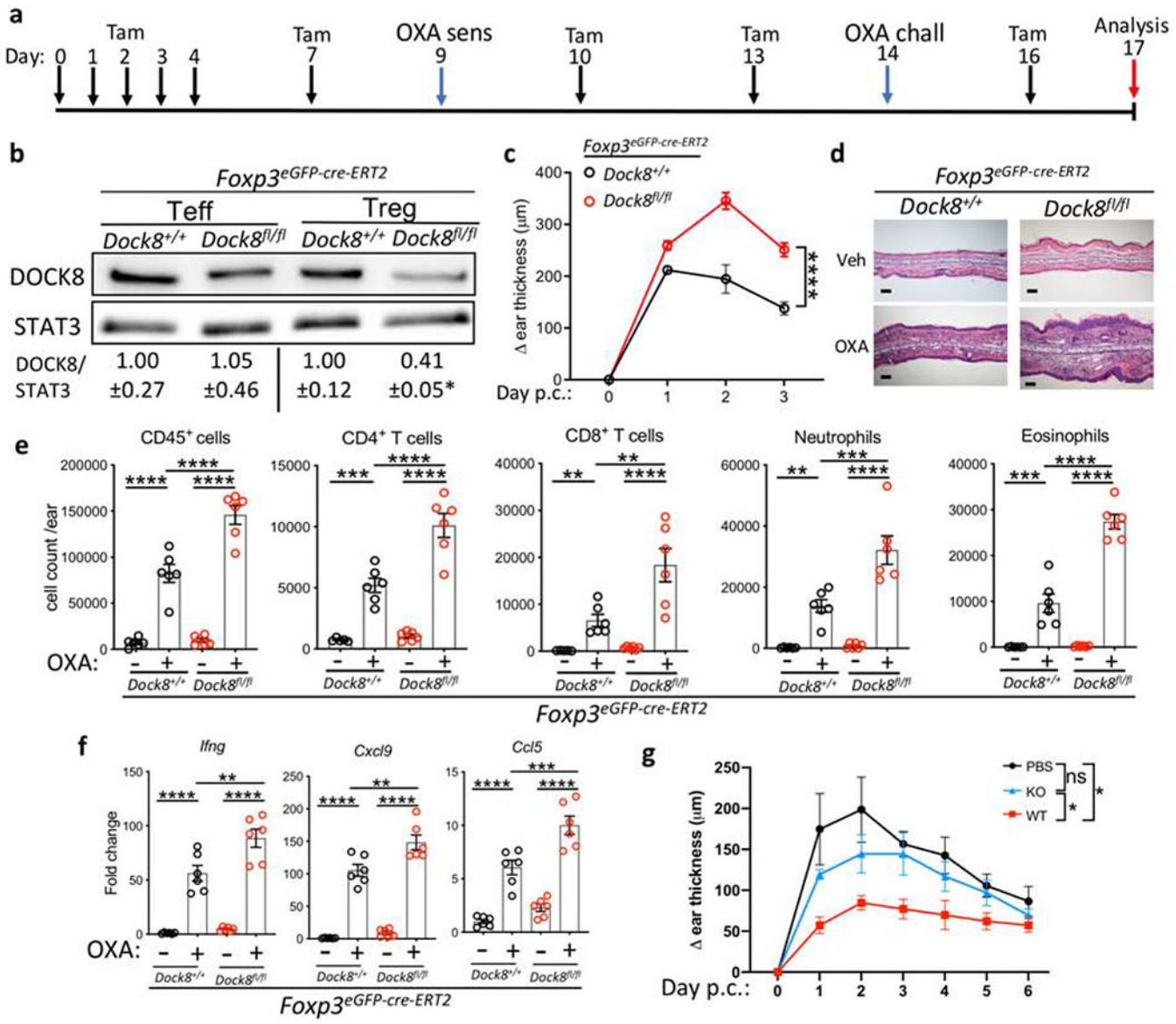

Figure 2. Prolonged CHS to OXA in mice with selective deficiency of DOCK8 in Tregs.

(**a**) Protocol of tamoxifen (Tam) treatment, OXA-sensitization (sens) and OXA challenge (chall). (**b**) Representative immunoblot (Upper panels) and quantitative analysis (Lower panel) of DOCK8 expression in $CD4^+FOXP3^-(GFP^-)CD25^-$ Teffs and $CD4^+FOXP3^+(GFP^+)CD25^+$ Tregs from tamoxifen-treated *Foxp3*$^{eGFP\text{-}cre\text{-}ERT2}$*Dock8*$^{flox/flox}$ mice and *Foxp3*$^{eGFP\text{-}cre\text{-}ERT2}$*Dock8*$^{+/+}$ controls. Values show DOCK8 expression relative to STAT3 expression in Teff and Treg cells normalized to the mean DOCK8/STAT3 ratio in controls. (**c**) Change in ear thickness post challenge (p.c.) with OXA versus vehicle in *Foxp3*$^{eGFP\text{-}cre\text{-}ERT2}$*Dock8*$^{flox/fox}$ mice and controls. (**d-f**) Representative photomicrographs of H&E stained sections, scale bars: 100 μm (**d**), cellular infiltration (**e**) and cytokine and chemokine expression relative to vehicle-challenged control (**f**) in ears on Day 3 post OXA (+) or vehicle (−) challenge. (**g**) Change in ear thickness post OXA challenge (p.c.) in OXA-sensitized *Dock8*$^{-/-}$ (KO) mice injected intra-dermally with Tregs from OXA-sensitized WT

or KO mice, or PBS immediately prior to OXA challenge. Symbols represent individual mice (n=6/group), bars display mean ± SEM. * p <0.05, ** p <0.01, *** p <0.001, **** p <0.0001, ns, not significant, by Student's t test (**b**), 2-way ANOVA for global significance (**c, g**) and 1-way ANOVA with Tukey's multiple comparison test for differences between groups (**e, f**).

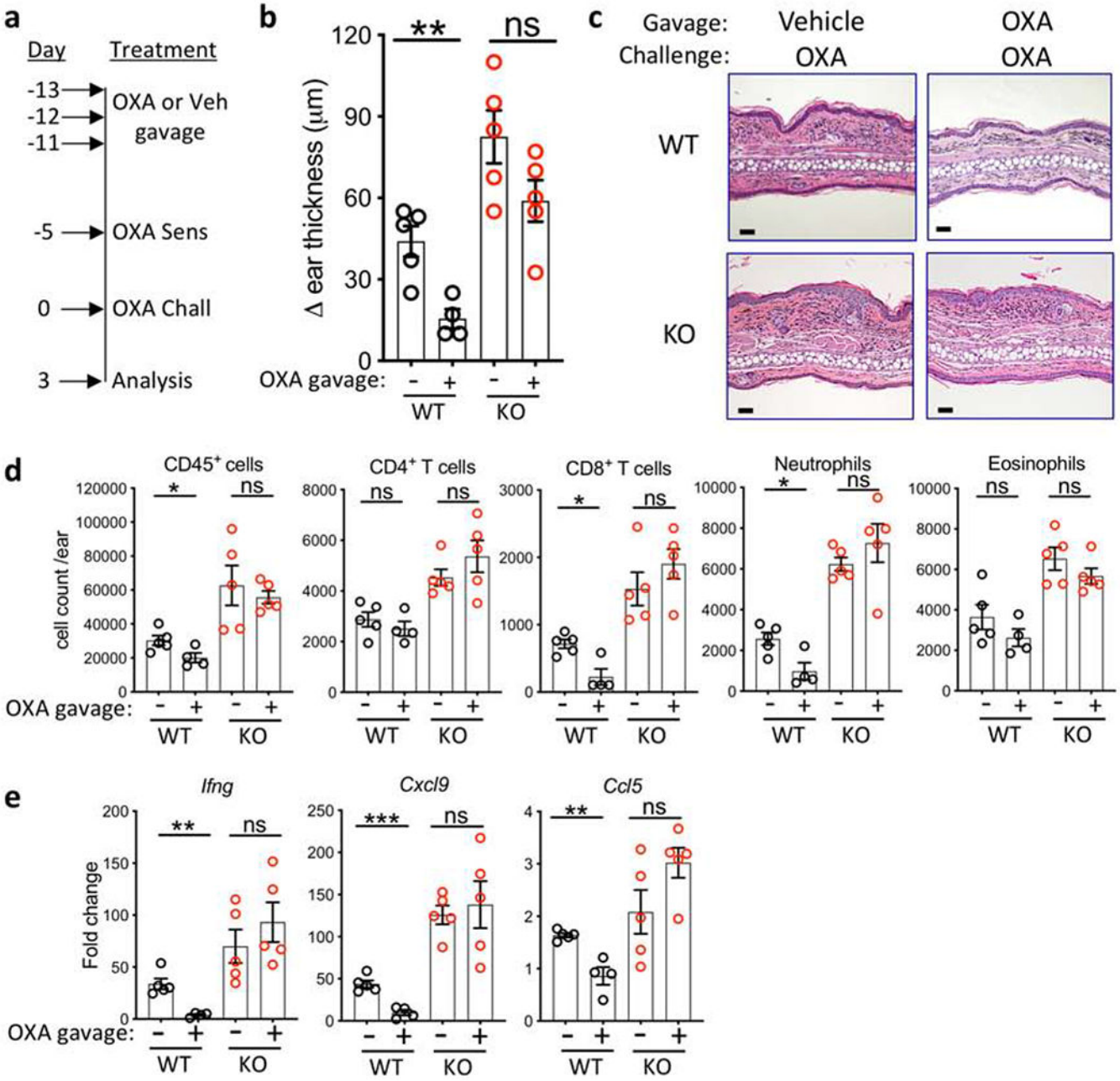

Figure 3. *Dock8*$^{-/-}$ mice are resistant to hapten-induced oral tolerance.

(**a**) Protocol of OXA induced oral tolerance. (**b**) Change in ear thickness post challenge (p.c.) with OXA versus vehicle in OXA (+) or vehicle (−) gavaged *Docks*$^{-/-}$ (KO) and WT mice. (**c-e**) Representative photomicrographs of H&E stained sections, scale bars: 50 μm (**c**), cellular infiltration (**d**) and cytokine and chemokine expression relative to vehicle-gavaged vehicle-challenged WT (**e**) ears from OXA-gavaged or vehicle-gavaged KO mice and WT controls. Symbols represent individual mice (n=4-5/group), bars display mean ± SEM. * p <0.05, ** p <0.01, *** p < 0.001, ns, not significant, by 1-way ANOVA with Tukey's multiple comparison test for differences between groups (**b, d, e**).

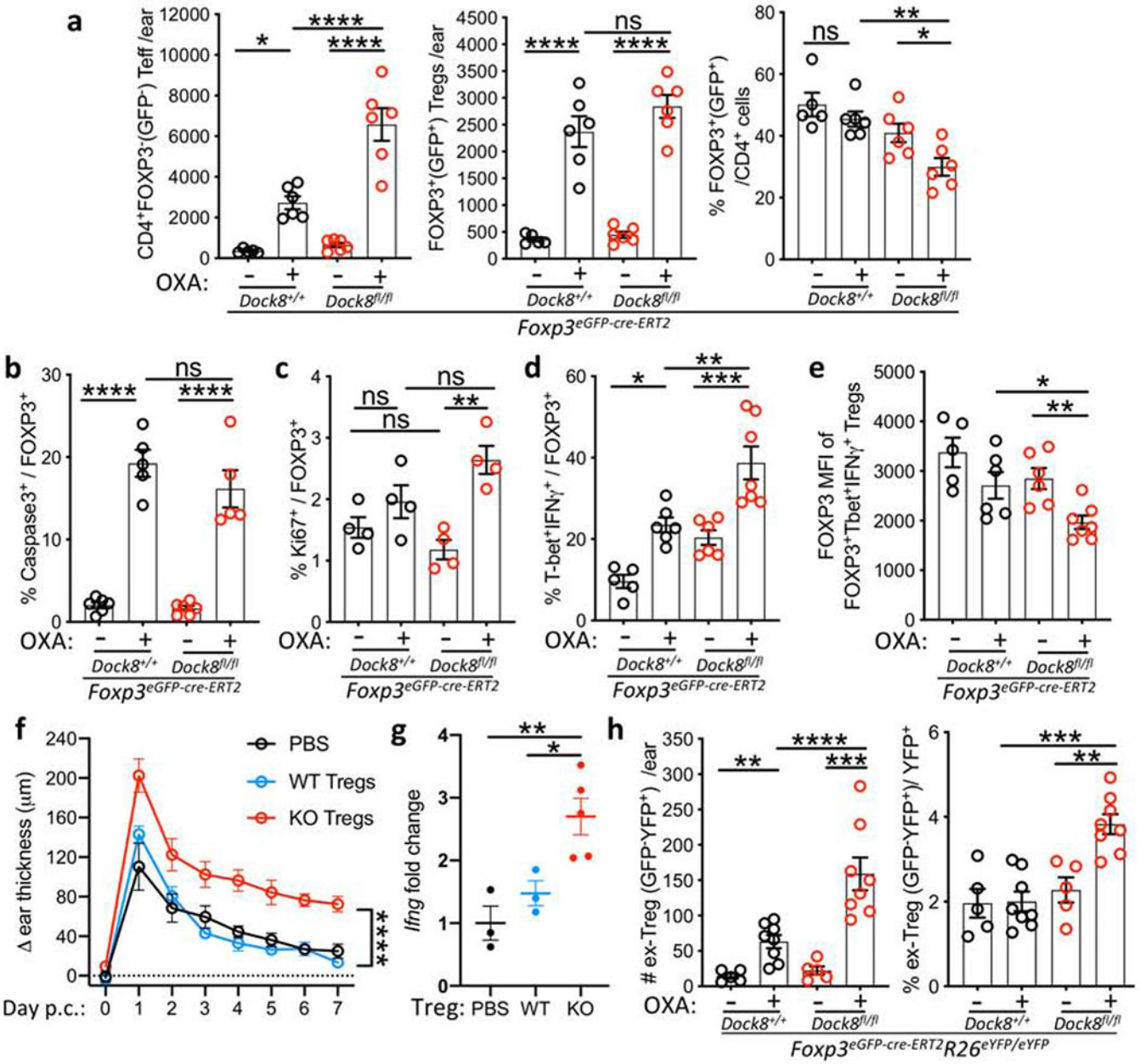

Figure 4. DOCK8 maintains Treg stability and fitness at sites of CHS driven skin inflammation.

(**a-e**) *Foxp3*$^{eGFP\text{-}cre\text{-}ERT2}$*Dock8*$^{flox/flox}$ mice and *Foxp3*$^{eGFP\text{-}cre\text{-}ERT2}$*Dock8*$^{+/+}$ controls were treated as in Figure 2a. (**a**) Numbers of CD4$^+$FOXP3$^-$(GFP$^-$) Teff (left), FOXP3$^+$(GFP$^+$) Tregs (middle), and percentage of Tregs among CD4$^+$ T cells (right). (**b-d**) Percentage of Caspase-3$^+$ (**b**), Ki67$^+$ (**c**) and T-bet$^+$IFNγ^+ cells (**d**) among FOXP3$^+$(GFP$^+$) Tregs. (**e**) MFI of FOXP3 in T-bet$^+$1FNγ^+FOXP3$^+$ Tregs. (**f, g**) Change in ear thickness post challenge (p.c.) with OXA (**f**) and *Ifng* expression on Day 7 p.c. relative to PBS injected controls (**g**) in naïve WT mice injected with naïve KO Tregs, WT Tregs or PBS immediately prior to OXA sensitization. (**h**) Numbers (left) and percentage of CD4$^+$FOXP3$^-$(GFP$^-$)YFP$^+$ ex-Tregs among total YFP$^+$ cells (right) isolated from ears of *Foxp3*$^{eGFP\text{-}cre\text{-}ERT2}$*R26*$^{eYFP/eYFP}$*Dock8*$^{flox/flox}$ mice and *Foxp3*$^{eGFP\text{-}cre\text{-}ERT2}$*R26*$^{eYFP/eYFP}$

Dock8$^{+/+}$ controls treated as in Figure 2a. Symbols represent individual mice (n=3-8/group), bars display mean ± SEM. * p <0.05, ** p <0.01, *** p <0.001, **** p <0.0001, ns, not significant, by 1-way ANOVA with Tukey's multiple comparison test for differences between groups (**a-e, g, h**) and 2-way ANOVA for global significance (**f**).